RADC-TR-90-29
Final Technical Report
February 1990

SINGLE MODE COMMUNICATION LINK

PCO, Inc.

Plessey Research Caswell Ltd.

Stephen R. Cole, D.C.J. Reid, R. Carpenter

APPROVED FOR PUBLIC RELEASE; DISTRIBUTION UNLIMITED.

Rome Air Development Center
Air Force Systems Command
Griffiss Air Force Base, NY 13441-5700

This report has been reviewed by the RADC Public Affairs Division (PA) and is releasable to the National Technical Information Service (NTIS). At NTIS it will be releasable to the general public, including foreign nations.

RADC-TR-90-29 has been reviewed and is approved for publication.

APPROVED: James R. Hunter

JAMES R. HUNTER
Project Engineer

APPROVED: John A. Graniero

JOHN A. GRANIERO
Technical Director
Directorate of Communications

FOR THE COMMANDER: B. G. Oaks

BILLY G. OAKS
Directorate of Plans & Programs

If your address has changed or if you wish to be removed from the RADC mailing list, or if the addressee is no longer employed by your organization, please notify RADC (DCLW) Griffiss AFB NY 13441-5700. This will assist us in maintaining a current mailing list.

Do not return copies of this report unless contractual obligations or notices on a specific document require that it be returned.

UNCLASSIFIED
SECURITY CLASSIFICATION OF THIS PAGE

REPORT DOCUMENTATION PAGE

Form Approved OMB No. 0704-0188

1a. REPORT SECURITY CLASSIFICATION UNCLASSIFIED	1b. RESTRICTIVE MARKINGS N/A
2a. SECURITY CLASSIFICATION AUTHORITY N/A	3. DISTRIBUTION/AVAILABILITY OF REPORT Approved for public release; distribution unlimited.
2b. DECLASSIFICATION/DOWNGRADING SCHEDULE N/A	
4. PERFORMING ORGANIZATION REPORT NUMBER(S) N/A	5. MONITORING ORGANIZATION REPORT NUMBER(S) RADC-TR-90-29
6a. NAME OF PERFORMING ORGANIZATION PCO, Inc. — 6b. OFFICE SYMBOL (If applicable)	7a. NAME OF MONITORING ORGANIZATION Rome Air Development Center (DCLW)
6c. ADDRESS (City, State, and ZIP Code) 20200 Sunburst St. Chatsworth CA 91311-6289	7b. ADDRESS (City, State, and ZIP Code) Griffiss AFB NY 13441-5700
8a. NAME OF FUNDING/SPONSORING ORGANIZATION Rome Air Development Center — 8b. OFFICE SYMBOL (If applicable) DCLW	9. PROCUREMENT INSTRUMENT IDENTIFICATION NUMBER F30602-86-C-0034
8c. ADDRESS (City, State, and ZIP Code) Griffiss AFB NY 13441-5700	10. SOURCE OF FUNDING NUMBERS

PROGRAM ELEMENT NO.	PROJECT NO.	TASK NO	WORK UNIT ACCESSION NO
62702F	4519	21	64

11. TITLE (Include Security Classification)
SINGLE MODE COMMUNICATION LINK

12. PERSONAL AUTHOR(S)
Stephen R. Cole, D. C. J. Reid, R. Carpenter

13a. TYPE OF REPORT	13b. TIME COVERED	14. DATE OF REPORT (Year, Month, Day)	15. PAGE COUNT
Final	FROM Feb 86 TO Nov 88	February 1990	52

16. SUPPLEMENTARY NOTATION
Plessey Research Caswell Ltd. is a subcontractor to PCO, Inc.

17. COSATI CODES			18. SUBJECT TERMS (Continue on reverse if necessary and identify by block number)
FIELD	GROUP	SUB-GROUP	Fiber Optic Coupler, Single Mode Fiber Optic Coupler; Fiber Optic WDM, Single Mode Fiber Optic WDM, Multichannel Single Mode Communication Link
25	05		
20	06	01	

19. ABSTRACT (Continue on reverse if necessary and identify by block number)

Optical fiber transmission has many features which make it very attractive for Military applications. Furthermore, single mode fiber is superior to multimode fiber in terms of bandwidth, attenuation, radiation resistance and cost. The benefits of single mode optical fiber transmission can be further enhanced with the use of Wavelength Division Multiplexing (WDM) technology in which multiple, independent optical signals may be simultaneously transmitted over a single fiber. This permits single fiber transmission of mixed signal traffic (e.g. digital data, voice, video, analog, etc.) as well as parallel digital traffic characteristic of computer data transfer. In addition, this technology creates new system design options and architectural flexibility for Local Area Networks (LANs). This technical report describes the design and development of the critical element for implementing such a communications link - a 16 channel single mode WDM. Specifically, it describes the development and performance of a grating-based single mode WDM system suitable for use with single longitudinal lasers (e.g. Distributed Feedback lasers (DFB's)). The 16 channel

20. DISTRIBUTION/AVAILABILITY OF ABSTRACT	21. ABSTRACT SECURITY CLASSIFICATION	
☒ UNCLASSIFIED/UNLIMITED ☐ SAME AS RPT. ☐ DTIC USERS	UNCLASSIFIED	
22a. NAME OF RESPONSIBLE INDIVIDUAL James R. Hunter	22b. TELEPHONE (Include Area Code) (315) 330-4092	22c. OFFICE SYMBOL RADC (DCLW)

DD Form 1473, JUN 86 — Previous editions are obsolete. — SECURITY CLASSIFICATION OF THIS PAGE
UNCLASSIFIED

WDM features channels with 3 dB bandwidths of 2.4 nM and separations of 7.2 nM. Any particular channel can be set to a precise wavelength due to the mechanical design features. End-to-End system channel insertion losses of 12.5 dB have been achieved with adjacent channel crosstalk of better than -25 dB.

TABLE OF CONTENTS

SUMMARY

A grating-based single mode fiber optic wavelength division multiplexing/-demultiplexing system suitable for use with distributed feedback lasers has been made. The mechanical design features the use of flexure mounts, which maximize the flexibility of final assembly and alignment and provide tunability of the unit. Sixteen channels with 3dB bandwidths of 2.4nm and separations of 7.2nm are available; any particular channel can be set to a precise wavelength. A channel insertion loss for the end-to-end system of 12.5dB has been obtained, and the adjacent channel crosstalk is typically better than -25dB for the end-to-end system.

1. INTRODUCTION

This work is a part of the "Single Mode Communication Links" program (Contract No. F-30602-86-C-0034). Some details of the work not included here may be found in earlier documents, CDRL Item A002 ("Design Plan") or Item A003 ("Test Plan").

2. OBJECTIVE

The aim was to build and carry out a preliminary optical assessment of a prototype 16-channel mux-demux device capable of single mode duplex operation centered on approximately 1550nm, and with channel widths and spacing appropriate for distributed feedback lasers.

3. DESIGN AND FABRICATION

3.1 PRELIMINARY DESIGN

Various options were examined in the "Design Plan", where it was concluded that from several points of view a grating-based design offered the best solution. This would employ a replica reflection grating in a near Littrow configuration with a high quality collimating lens and a lithium niobate-based waveguide concentrator to increase the channel packing density. Unlike earlier designs, the common (i.e., input/output) channel would be accessed directly and not through the waveguide in order to reduce insertion loss. Figure 1 illustrates the principle.

3.2 DETAILED DESIGN

Starting with the need to (1) minimize waveguide fiber/field mismatch at the fiber/concentrator interface and (2) to achieve 25dB or greater channel isolation, a beam width of approximately 8 micron and separation of 25 micron would be required. A channel width of about 3nm was needed to allow for variations in laser wavelengths so a channel spacing of around 9nm was indicated.

The required characteristics of the lens and the grating could be related to these parameters through

$$d \cos \theta = fC/D \qquad (1)$$

d = grating spacing D = waveguide separation

f = lens focal length θ = diffraction angle (normal incidence)

C = channel spacing

Excessive loss would be introduced if the numerical aperture (NA) of the lens was smaller than that of the waveguides or common fiber (approximately 0.1). Hence, the lens would have to be at least F/5 (F-value = $\frac{1}{2NA}$). The resolution (R) of the grating needed to separate out the channels can be related to the lens and waveguide/fiber (NA) through

$$R = 2(f)(G)(n)(NA_f) \qquad (2)$$

where G = groove density

n = grating order

NA_f = fiber numerical aperture

A suitable grating could be selected and the corresponding lens focal length calculated from equation (1). A first order normal incidence grating blazed to give a diffraction maximum at 1550nm was required. Closest to this was a commercially available 200 groove/mm grating (Milton Roy) blazed for 1700nm; the diffraction efficiency was nearly as good at 1550nm. The diffraction angle at 1550nm was 8.9° and a focal length of 13.2nm was indicated by substituting in the equation. With this lens and grating the resolving power of 3nm would easily separate the 9nm channels.

3.3 LENS EVALUATION

A 13.2 mm focal length lens was unavailable from normal sources as a stock item. A custom built lens could have been obtained, but not within the timescale of the program. The first alternative considered was to use a standard objective and tune the focal length with a supplementary positive or negative lens. The supplementary lens could be in contact with or separated

from the objective. With the in-contact approach, there were practical difficulties with surface scuffing and provision of suitable anti-reflection coating. With the out-of-contact approach, the provision of suitable mountings was a problem. Minimizing spherical aberration and coma was possible for fixed focal length lenses to enable the diffraction limit to be approached, but impossible for a separated lens combination of varying focal length.

For these reasons it was preferable to use a single lens or compound objective. A suitable lens had to be obtained. Immediately available were lenses manufactured by Ealing Optical plc and by Optics for Research. Two of these were IR objectives, while the third, a single element 'best form' lens, had a focal length close to that required.

In order to assess the lenses, a linear array of 10 single mode fibers (50 micron pitch, 10 micron core diameter) and a front-silvered mirror were used instead of the concentrator and grating respectively, since these were unavailable at the time. The array and mirror were placed in the focal planes of the lens. The system was aligned by launching a HeNe laser beam into an outside fiber of the array and visually maximizing the light reflected and then transmitted into the other outer array fiber. To do this, the mirror tilt and array position were adjusted, the latter with piezo-driven adjusters. A 1530nm temperature-stabilized laser was substituted and the output, monitored with a germanium detector, maximized. Intermediate outputs were examined by altering the mirror tilt and the values maximized and recorded. Differences in the corresponding axial positions of the array were also noted. Figure 2 details these results in terms of insertion loss, measured with respect to the direct beam from the fiber array, against off-axis position. For a meaningful comparison, the data from the single element lens which was not A-R coated was corrected to allow for surface reflections. There was no significant shift in the position of the focal plane in any of the lenses.

The table below gives details of the lenses together with measurements of the single-pass transmission loss obtained by substituting a large-area detector for the grating.

Table 1

Lens Details

Manufacturer	Type	Transmission Loss (dB)
Optics for Research	I.R. Obj. LMO 10X	1.0
"	'Best Form' LLU-13-15	0.3
Ealing	I.R. Objective	0.3

The results clearly demonstrated the superiority of the Ealing objective lens. The loss through the Optics for Research objective suggested non-optimization of the A-R coatings. The flatness of the loss characteristic over the relatively wide field examined in the focal plane indicated that there would be no difficulty in obtaining adequate performance over the smaller field of the multiplexer, provided that the lens aberration introduced through focal length adjustment was not significant.

3.4 FOCAL LENGTH TOLERANCE

Equation (1) shows that since d, D and cos θ are system constants, the product of the lens focal length and the channel separation is a constant. A small increase in the design focal length produces a corresponding decrease in the channel separation. This does not affect multiplexing, but is very significant in a combined mux-demux system. Across N channels, the total center-to-center wavelength range = (N-1) x channel spacing, and the focal length tolerance, Δf, between a pair of lenses used in mux and demux, can be expressed as

$$\Delta f = \left(\frac{1}{N-1} \right) \frac{\Delta C}{C} \qquad (3)$$

where ΔC is the permissible variation in C, the channel spacing.

Hence, the fractional change in focal length is the same as the change in AC expressed as a ratio of the total channel bandwidth. For a channel spacing of 9nm and a permitted change of 1nm in the channel center position, the overall tolerance on focal length is 1 part in 145 or less than ±0.7%.

3.5 LENS SPECIFICATION

Summarizing, the lens requirement was for a high quality IR F/5 or faster lens of focal length 13mm. Although the absolute focal length was not critical, mux and demux lenses needed to be matched to within ±0.7% in focal length. Trials of standard lenses indicated that an Ealing IR lens gave a very good performance. The manufacturer could not provide a lens of absolutely the correct focal length, but was willing to match pairs of lenses to a focal length tolerance of ±1% with an appropriate coating. Furthermore, the lens could be obtained with cements suitable for elevated temperatures and these were ordered.

3.6 DIFFRACTION GRATING

As stated earlier, 200 groove/mm blazed gratings manufactured by Milton Roy were selected. The efficiency quoted was 88% at λ=1.55 micron. The manufacturer would not guarantee operation at elevated temperatures, but confirmed that they had been used between -100 and +85C. The epoxy used in replication is manufactured by Shell ('Epon').

3.7 WAVEGUIDE CONCENTRATOR

A separate assessment was made of the lithium niobate waveguide concentrator to optimize the parameters from the point of view of insertion loss an crosstalk. The mask designed for the fabrication included a selection of waveguide widths (6.5, 7.5 and 8.5 micron) and waveguide separations (24, 25, 26, 27 microns) to permit the comparison. Waveguide pitch at the wide end was chosen to be 128 micron to allow for the glue in mounting 125 micron diameter single mode fiber. A symmetrical waveguide pattern was chosen so that the

central guides were straight. The bend loss of the outer guides was kept small by ensuring that all guide radii were at least 40mm. At the narrow end the guides were limited to 1mm in length to reduce cross coupling. Eighteen guides were incorporated into the concentrator patterns to allow for possible channel failure. The frame width, larger than the pattern to ease handling, was 5mm and the length was 15mm. The lithium niobate slice thickness was 1mm. Standard lithographic and diffusion procedures were used to produce these concentrators. The various patterns were examined optically to decide which matched most closely the array fiber. Guides 6.5 micron wide on 25 or 26 micron pitch resulted in a guide loss of 0.5dB in the outer channels, after allowing for interface reflections. Crosstalk values below 30dB were achieved. Concentrators with these guides were A-R coated at the air interface with a quarter wave layer of silica to reduce loss.

3.8 FIBER ARRAYS

For reasons which will be discussed later (Section 3.9), fibers cabled and connectorized at one end were used. Matching the fiber pigtails to the wide end of the waveguide array was accomplished with silicon V-grooves. The method of producing these grooves is well known and involves photolithography on a well aligned (100) silicon slice with orientation dependent etching through a mask formed in the oxide layer.

The fiber ends of the connectorized cables were threaded through the plug used to obtain the hermetic seal and positioned in the V-grooves (Section 3.9). Adhesive was applied and hardened before the fiber ends were polished. Figure 3 shows one of the 18 fiber arrays fabricated using this technique.

The single input/output fiber in the plane of the concentrator was also located within a silicon V-groove. To assist with the initial optical alignment of the system, two adjacent V-grooves parallel to this groove were also incorporated to retain multimode fibers. The cabled input/output fiber was also passed through the sealing plug before the 3-fiber array was produced as described above. In this case the silicon chip was 5mm long and 5mm wide.

3.9 ASSEMBLY CONCEPTS

The original intention was to glue the various components in position after careful alignment with external manipulators. Detailed examination indicated that this technique was not viable for a prototype unit, because of the exceedingly fine adjustment needed, the number of degrees of freedom required and the difficulty of holding the components firmly in close proximity. There was also the severe limitation of the lack of tuning after assembly. Failure to set the channel position precisely or movement during adhesive hardening would be catastrophic and would require the recovery of the expensive components. This would probably prove to be difficult.

For these reasons the original design concept was modified and an assembly designed which would permit in situ alignment and adjustment of any channel to a particular wavelength within the range. This would introduce flexibility and enable a single laser to be used for assessment of any channel. Of major concern was the sensitivity of the assembly to temperature. Additional requirements were to ensure environmental protection against dust and moisture and to design the assemblies to be as shock-proof as possible.

Very small adjustments to mirror tilt (minutes of arc) and lens focusing (microns) would be needed to obtain optimum alignment of the optical system. To accomplish this with conventional stages would require a very bulky and temperature sensitive assembly. There was a possibility of using stages which depend on flexure to produce the very sensitive but limited movement needed. Tilt can be produced in this way as shown in Figure 4. The full potential of this design does not seem to have been realized, since only one design is at present marketed (Newport Corporation).

Some preliminary tests were made with the system described earlier for lens assessment, but with the mirror attached to a Newport mount. Although the mounts lacked adjustment sensitivity, it was possible to align the reflected beam into each array fiber in turn. However, the commercially available flexure mount was not obtainable in low expansion alloy nor was the design suitable.

The adjustments designed into the systems which are shown in Table 2, are discussed in detail below.

TABLE 2

BUILT-IN MULTIPLEXER ADJUSTMENTS

Component	Degree of Freedom	Method	Reason
Concentrator	Axial shift.	Slide	Coarse focus
	Tilt of waveguide plane.	Single flexure mount	Alignment perp. to grating grooves
Lens	Axial shift. Tilt of lens axis about main optical axis.	Two parallel flexure mounts	Fine focus -
Grating	Two orthogonal tilts.	Two orthogonal flexure mounts	Channel wavelength adjustment. Alignments perpendicular to waveguide array axis.

The flexure mounts were individually designed and they incorporated adjustment screws having a very fine 0.35mm pitch to increase sensitivity. To limit thermal effects the mounts were made of invar. The spring flexures and screws were steel of approximately the same expansion and were to this extent self-compensating. A very reliable method was needed for joining the invar plate to the steel spring. Conventional spot welding proved to be unsuccessful but laser spot welding provided a weld of great integrity as indicated by metallurgical examination. The flexure mounts were manufactured in the workshop at Plessey Caswell.

Means of integrating the various components were considered in detail. A light rigid mounting insensitive to temperature changes was the main requirement. This criterion was not met by a conventional mini optical bench. The design

was based on that used for Fabry-Perot etalons.

Four ground alignment rods precisely located and screwed into end plates formed a rigid structure. One end plate was also used for mounting the grating flexure mounts. An intermediate plate was located on the four rods and axially positioned and clamped via grub screws impinging on short flats on the rods. This intermediate plate was used to support the lens flexure mounts and was also bridged to the second end plate with a plate which served as a mount for the concentrator assembly. All these plates and the alignment rods were made of invar to minimize thermal expansions.

The critical adjustments for the grating were tilts in the two planes parallel and perpendicular to the grooves and these were provided by the flexure plates, arranged as shown in Figure 5.

The flexure mount used for the lens is illustrated in Figure 6. Tilt produced between the end plates was balanced by adjusting both screws to leave axial displacement alone. Although the lens cements would withstand 85C, the effect of temperature on focal length was unknown. This effect could not be investigated at the time owing to the long delivery schedule for the lenses. A re-entrant mounting was used to attach the lens to the flexure mount; this helped to reduce both expansion effects and the overall length of the assembly.

Figure 7 shows the flexure mount used for the concentrator. This enabled a slight tilt adjustment to be made to the plane of the waveguide array and compensated for any slight misalignment of the grating. A nickel-plated mild-steel plate was used as a common substrate for the concentrator and fiber array, since the expansion coefficient of mild steel closely matched that of lithium niobate in directions perpendicular to its thickness. The mild-steel plate was screwed to the upper half of the invar flexure mount. The method of attachment was designed to minimize the effect of expansion differences between invar and mild steel on the position of the front-face plane of the waveguides. The bottom half of the flexure mount was slotted to permit coarse axial adjustment of the entire concentrator assembly with respect to the invar bridging plate into which it was screw mounted.

Ways in which the fibers could be brought from the multiplexer and connected into a system were considered. None were entirely satisfactory. The multiplexer needed to be case-mounted for protection. Fibers alone were most suitable from the hermetic sealing point of view, but would require welds or splices for system connection.

The use of connectors was much preferred from the convenience and robustness points of view, but low-loss single mode fiber connectors with hermetic sealing were unavailable. However, connectorized cables with fiber tails were chosen as the best compromise, but complete environmental protection was then impossible. Physical-contact (P.C.) connectors (Amphenol) were selected for low loss. These had an upper temperature limit of 70C. The bundle of nineteen close-packed cables was sealed with an epoxy recommended by the cable manufacturer into a cylindrical plug, which was itself sealed with an O-ring as it passed through the wall of the case. It might have been possible to prevent or reduce moisture ingress through the cable from the connector by sealing the fibers into the cable casings at the multiplexer end with silicone rubber or similar encapsulant, but the time available did not permit this avenue to be explored.

A mechanical clamp, attached to the invar assembly was designed to hold the cable bundle rigid and prevent strain from being transferred to the concentrator assembly. This clamp could be detached and used for holding the fibers during assembly of the V-groove array. Between the V-groove array and the mechanical clamp the fibers changed from a linear to a cylindrical form.

The multiplexer and associated connectors could be separated completely from the case. Freedom of access to all the setting screws on the assembly was consequently ensured. Rubber pads located on the invar end plates provided the means for positioning the assembly within the case. Finally, an O-ring-sealed lid made the entire unit demountable.

3.10 ASSEMBLY

The assembly of the fiber array to the concentrator was critical as any

misalignments would introduce very significant loss. The common nickel-plated mild-steel baseplate was screwed horizontally via an adapter to a stack of precision stages giving translation and tilts in all three planes. The lithium niobate concentrator was spaced from the baseplate by short lengths of fiber and gently biased into contact with a lightly sprung rubber pad. A thin nickel-plated disk of soft iron was glued to the top surface of the silicon V-groove array. An arm carrying a small ferrite disk magnet, to couple to the soft iron disc, was designed to position the silicon array in close proximity to the waveguides. This arm was connected to very sensitive X, Y, Z piezo-driven stages. The height difference between the axes of waveguides and fibers was accommodated by milling away the baseplate underneath the lithium niobate. The height difference was about 50 micron less than actually needed; this permitted tapered fibers to be inserted between the silicon and the baseplate. The purposes of the fiber wedges was to provide a positive location for the silicon and room for an adhesive bead. Initially the fiber and waveguide arrays were positionally matched as closely as possible under a microscope.

A dual wavelength optical system was provided for each outer fiber (nos. 1 and 18) of the silicon V-groove array. This consisted of a visible beam launched into the fiber from a He-Ne laser and an I-R beam from an electronically chopped and thermally stabilized pigtailed 1550nm laser. The chopping frequencies for the two channels were different to enable the signal levels of a composite signal to be separated with lock-in amplifiers. The dual wavelengths were introduced into the fiber cables via fiber couplers. A horizontally mounted microscope (x70 total magnification) was used to view the narrow end of the waveguide concentrator image. A preliminary alignment of the outer channels of the waveguides with the outer array fibers was made using visible light. With IR substituted the maxima were by no means as distinct as anticipated. An iris of small diameter in the image plane immediately in front of the detector eliminated some of the scattered light from the concentrator substrate, but the resolution still did not permit more sensitive alignments than those that were possible with the visible light. Indeed, after equalizing the visible output intensities from the illuminated array fibers, the two arrays could be aligned very closely by adjusting the tilt micrometers until the two spots disappeared simultaneously when the array planes were moved

perpendicular to each other. Fine tuning was then possible using the IR beams.

A small amount of UV curing adhesive ("Norland") was drawn by capillary action between the fibers and waveguides and the IR outputs checked before the adhesive was hardened. A light-curing resin (ICI LTd.) was used to cement the concentrator and silicon array to the baseplate; the 488nm fiber transmitted radiation from an Argon-ion laser provided an intense and convenient source. Care was taken to limit the adhesive to the edge of the fiber array as silicon absorbs this wavelength. After curing, the assembly with the cables held by the mechanical clamp was removed from the jig and carefully fitted to the main invar assembly.

The silicon V-groove chip containing the cabled input/output fiber and two multimode fibers was carefully held with a spring-loaded pad on top of the concentrator and aligned under a microscope so that the front surfaces of fiber and waveguides were co-planar. The light-curing resin was applied to the side edges of the chip and immediately cured. Great care was taken to prevent any adhesive from reaching the front surfaces of the waveguides.

The compactness of the design did not permit direct access to the lens. The flexure mount had to be removed from the main unit and the lens attached before reassembly. Access to this flexure mount was possible only after removing the grating mounting plate.

The grating was mounted against a wedge-shaped plate (wedge angle = diffraction angle at 1550nm), which was then bolted to the grating flexure mounts. Care was taken to prevent stressing the grating, a small pad of silicone rubber adhesive was used at the center of the silica backing plate to provide resilience. The grooves were set parallel to the wedge and the grating very gently pressed into contact with the invar surface. After the silicone rubber had cured, a thin fillet of adhesive (UV curing) was used around the edges to provide rigidity.

Figures 8, 9, and 10 show respectively an assembly before and after case mounting and the hermetically sealed unit with its associated connectors.

4. SYSTEM ALIGNMENT

Alignment was carried out in several stages. In general it was easier to align the components initially with visible light. The dual wavelength, visible and IR, system described in section 3.10 proved to be very suitable for doing this. The grating mount was removed, light was introduced through one of the central fibers of the array and the relative positions of the lens and waveguide array adjusted so that collimated light was transmitted. The grating mount was replaced, but with a front-silvered mirror attached in place of the wedge-shaped plate. The mirror tilt was adjusted until the reflected spot, viewed with a microscope, was visible close to the central guides. The fiber ends at the connectors were observed and very small adjustments made to the mirror and to the focus until the output from the illuminated fiber was at a maximum.

The IR beam was substituted and the same output, monitored with the large-area detector and lock-in amplifier, adjusted with the focus and tilt movements to a maximum. The mirror tilt was adjusted to illuminate the other fibers in turn and the lens and mirror adjustments altered until the outputs from the two extreme fibers were both at a maximum. Finally, the tilt was readjusted so that the illuminated output fiber was one adjacent to the central input.

The mirror was replaced with the grating and the outputs from several central fibers examined simultaneously. A very small signal was generally detectable. If not, very small adjustments were made to the mirror tilt until an output was observed. The procedure described above to maximize the output, and then to check that the extreme fiber outputs, was repeated. In this case small adjustments were also needed to the tilt of the waveguide array to compensate for slight misalignment in the direction of the grating grooves.

The diffracted beams were at this stage coincident with the waveguide array, however, they needed to be in the plane of the output fiber. The waveguide closest to the output fiber was illuminated and the outputs from the two multimode fibers of the output array were monitored. The grating was tilted along the axis parallel to the plane of the waveguides, and the angular rotation of the adjustment screw on the flexure mount was noted. If no output

could be detected, a very small alteration was made to the tilt in the other plane and the scan repeated until an output was located. This output was maximized by using the grating tilts alone. The position of the particular multimode fiber illuminated was known with respect to the single mode output fiber, so the direction of grating tilt to diffract the beam into the output fiber could be deduced. The signal in this fiber was maximized by using the grating tilt.

After these procedures had been completed, the light direction was reversed and the outputs from the array examined in turn by tilting the grating about an axis perpendicular to waveguide plane. In the two multiplexers there was one channel in each array through which no light was transmitted.

Ideally two lasers with a wavelength difference equal to the center-to-center wavelength spacing of the outside channels were needed to complete the alignment. By adjusting the concentrator tilt, the relative orientation of the grating and waveguide planes could then be set precisely. However, only one laser, furnished by Plessey Caswell, was available for final alignment and another method had to be used. The two outer channels were illuminated in turn and after adjustment the maximum transmissions were noted. With one output at a maximum, the beam was shifted to the other outer channel using only the grating adjustment which moved the beam in the plane of the waveguides. The other grating tilt adjustment and the waveguide tilt were then adjusted to bring the output nearer to the noted maximum. This procedure was repeated step-by-step until both outputs could be tuned to their respective maximum with grating tilt in the plane of the waveguide alone.

5. OPTICAL CHARACTERIZATION

5.1 EQUIPMENT

A high-resolution Bentham monochromator of 300cm focal length illuminated with mechanically chopped radiation from a stabilized tungsten lamp was used as the input in the wavelength-scanning measurements described below. The monochromator output was intercepted with the fiber end of a connector pigtail positioned in the plane of the output slit. This connector output was adapted

to mate with any connnectorized end of the multiplexer. A similar arrangement was used to adapt to the pigtailed small-area InGaAs PIN diode used as the detector. The detector output was fed through a current preamplifier to a lock-in amplifier. The amplifier output was measured on a digital voltmeter or connected into a recorder.

In other cases IR lasers provided by Plessey Caswell were used and the outputs detected by large area Ge detectors with associated lock-in amplifiers.

5.2 NEAR-END CROSSTALK

A Caswell DFB laser was connected to channel 15 of assembly I and the grating tilt adjusted until the signal from the output fiber was maximized. The signals from channels 14 and 16 were monitored individually with the detector connected to a high sensitivity lock-in amplifier. Both these signals were at least 65dB down with respect to the input to the multiplexer.

5.3 FAR-END CROSSTALK

The light direction was reversed by connecting the laser to the input/output fiber. Channels 14 and 16 were again monitored, both signals were 60dB or more below the input level.

5.4 POLARIZATION EFFECTS

During the preliminary assessment of the concentrator chips, linearly polarized light in the two waveguide planes had been used to see whether these affected the transmission loss. This loss was only 0.5dB and difficult to measure with the system used. Differences in loss between the two excited guide modes were estimated to be below 0.25dB.

The polarization sensitivity of the grating was also measured at an earlier stage by diffracting a collimated 1550nm laser beam from the grating onto a large-area detector. A half-wave plate was inserted into the collimated beam and rotated to rotate the plane of vibration of the light. Very small

variations were observed in the detector output. These were 5% or less measured on a digital voltmeter. The diffraction efficiency at this wavelength was 85% (0.7dB loss).

As expected, there was no change in the corresponding output channel level, when the polarization state at the input was altered by rotating the connector coupling to the laser.

5.5 ABSOLUTE CHANNEL SETTING

Only one DFB laser (Plessey) was available for general characterization. However, for the absolute setting of channel wavelengths, channel 7 was adjusted to match that of an existing laser at RADC (1532nm). The various setting screws were locked with adhesive after the adjustment had been completed. This procedure was carried out on both units.

5.6 MONOCHROMATOR RESPONSE

This was determined initially by directly connecting the connector output of the monochromator to the detector and recording the lock-in amplifier output as the monochromator was wavelength scanned. The stabilized lamp output and fiber position at the exit slit were left untouched during subsequent measurements.

5.7 CHANNEL BANDWIDTH

The monochromator was connected to the input channel and channel 3 (assembly I) was monitored on the recorder during a wavelength scan. The channel response curve obtained is shown in Figure 11. The output response of the monochromator was constant over the channel wavelength so the half-power point channel width could be determined directly. The measured value of 2.9nm was widened by the monochromator resolution (0.5nm). Hence, the actual channel bandwidth of the coupler alone was about 2.4nm.

5.8 CHANNEL LOSS AND WAVELENGTH SEPARATION

The input channel was connected to the monochromator and the output array

channels connected in turn to the detector during the wavelength scan. A series of peaks corresponding to the individual channels was obtained. These were normalized with the monochromator response curve. A slower scan was used to located the individual peak maxima so that the precise output levels and wavelengths could be measured.

The loss for individual channels and the center channel wavelengths were determined for both multiplexers using this technique. Figure 12 shows the experimental wavelength response curves for the multiplexers. Figure 13 gives this data in the form of a loss histogram together with similar data from the other multiplexer. Table 3 gives the central channel wavelengths for each of the multiplexers and the derived channel spacings. Figures 12 and 13 also include loss measurements made on the units combined. For ease of measurement all the channels (1-18) were cross connected in the two units, the output of the monochromator was connected to one of the input/output channels and the other input/output channel to the detector. One multiplexer was left in the laboratory for four days and then without adjustment remeasured, and no significant changes were observed.

5.9 TEMPERATURE MEASUREMENTS

Measurements of loss and channel center wavelengths were made on one multiplexer at spot temperatures. The elevated temperature was produced with an oven. The lower temperature was produced by using a freezing mixture with the multiplexer suitably protected. After the temperature had been raised to 40C, the channel losses were remeasured at room temperature to check that no catastrophic increase had occurred. The multiplexer temperature was then raised to 50C, where the loss and wavelength measurements were taken. The device was then cooled to room temperature where the loss measurements were repeated. Finally, the multiplexer was cooled to 0C and the loss and wavelength measurements were repeated. Table 4 shows the set of loss data taken during the course of these cycles and include the earlier data for comparison. The corresponding wavelength data is contained in Table 5.

TABLE 3

WAVELENGTH MEASUREMENTS

Channel	Assembly I		Assembly II	
	Wavelength	Channel Spacing	Wavelength	Channel Spacing
1	1489.5		1488.9	
		7.1		7.2
2	1496.6		1496.1	
		7.3		7.3
3	1503.9		1503.4	
		7.3		7.2
4	1511.2		1510.6	
		7.4		7.5
5	1598.6		1518.1	
		6.9		7.1
6	1525.5		1525.2	
		6.7		7.3
7	1532.2		1532.5	
				7.2
8			1539.7	
9	1546.8		-	
		7.5		
10	1554.3		1554.3	
		7.2		7.2
11	1561.5		1561.5	
		7.1		7.1
12	1568.6		1568.6	
		6.9		7.3
13	1575.5		1575.9	
		7.3		7.5
14	1582.8		1583.4	
		6.9		7.6
15	1589.7		1591.0	
		7.6		6.7
16	1597.3		1597.7	
		6.9		7.1
17	1604.2		1604.8	
		7.0		7.0
18	1611.2		1611.8	

TABLE 4

EFFECT OF TEMPERATURE CYCLING ON LOSS (ASSEMBLY I)

Channel	Insertion Loss L or ΔL (dB)								
	Early data L_0	After 40C Cycle L_1	At 50C L_2	ΔL L_2-L_1	After 50 Cycle L_3	At 0C L_4	ΔL L_4-L_3	After 0C Cycle L_5	ΔL L_5-L_0
1	9.1	8.7	9.9	1.2	8.8	9.2	0.4	8.3	-0.8
2	8.3	8.1	9.7	1.6	8.0	8.9	0.9	8.0	-0.3
3	7.8	7.5	9.1	1.6	7.9	8.3	0.4	6.5	-1.3
4	7.1	6.9	8.6	1.7	7.5	7.8	0.3	6.5	-0.6
5	6.6	6.8	7.6	1.8	7.4	6.8	-0.6	6.6	0
6	6.2	6.0	7.3	1.3	6.2	7.6	1.4	6.7	+0.5
7	8.6	8.7	10.9	2.2	8.6	10.9	2.3	9.0	+0.4
8	-	-							
9	6.5	5.9	7.5	1.6	6.8	6.9	0.1	5.9	-0.6
10	6.7	6.1	7.8	1.7	7.3	8.0	0.7	5.7	-1.0
11	5.8	5.8	6.3	1.1	5.9	6.1	0.2	5.4	-0.4
12	6.5	5.5	7.2	1.7	6.2	7.8	1.6	5.9	-0.6
13	5.7	6.0	7.0	1.0	6.3	7.0	0.7	6.7	+1.0
14	5.9	6.0	7.3	1.3	6.3	7.9	1.6	7.2	+1.3
15	5.9	6.2	7.5	1.3	6.0	8.1	2.1	6.7	+0.8
16	6.3	6.2	8.0	1.8	6.5	8.6	2.1	6.3	0
17	6.8	6.8	8.4	1.6	7.1	8.9	1.8	7.2	+0.4
18	7.8	7.7	9.8	2.1	8.2	10.0	1.8	8.0	+0.2

TABLE 5

TEMPERATURE EFFECTS ON CENTRE CHANNEL WAVELENGTHS (ASSEMBLY I)

Channel	20C	50C	$\lambda_{20}-\lambda_{50}$	0C	$\lambda_{20}-\lambda_{0}$
1	1489.5	1491.7	-2.2	1489.9	-0.4
2	1496.6	1499.0	-2.4	1497.3	-0.7
3	1503.9	1506.0	-2.2	1504.2	-0.3
4	1511.2	1513.2	-2.0	1511.6	-0.4
5	1518.6	1520.6	-2.0	1519.0	-0.4
6	1525.5	1527.5	-2.0	1525.8	-0.3
7	1532.2	1534.6	-2.4	1532.8	-0.6
8	-	-	-	-	-
9	1546.8	1549.2	-2.4	1547.2	-0.4
10	1554.3	1556.3	-2.0	1554.4	-0.1
11	1561.5	1563.8	-2.3	1561.9	-0.4
12	1568.6	1571.0	-2.4	1569.2	-0.6
13	1575.5	1578.2	-2.7	1576.0	-0.5
14	1582.8	1585.0	-2.2	1583.1	-0.3
15	1589.7	1592.5	-2.8	1590.4	-0.7
16	1597.3	1599.9	-2.6	1597.6	-0.3
17	1604.2	1606.7	-2.5	1604.6	-0.4
18	1611.2	1614.2	-3.0	1611.5	-0.3
Average channel spacing:	7.16	7.20		7.15	

TABLE 6

WDM INSERTION LOSS ESTIMATES

Location	Source	Loss (dB)
Connector link to fiber array	Connector	0.3
	Fiber array matched to adhesive	0
Array to concentrator	Adhesive to concentrator	0.15
	Field mismatch fiber to waveguide	0.4
	Waveguide transmission	0.5
Concentrator to lens	Concentrator air interface. Partly A-R coated.	0.1
	Lens. Fresnel loss surfaces. 1/2% each surface.	0.13
Lens to grating	Measured efficiency 85% at 1550nm	0.7
Grating to lens	Fresnel loss at lens surfaces	0.13
	Aberration (image degradation)	0.7
Lens to connector	Field mismatch	0.4
	Fiber-air interface	0.15
	Connector	0.3
	TOTAL	4.0

6. DISCUSSION

6.1 INSERTION LOSS

Table 7 shows channel insertion losses measured from connector through to connector, varying between 5.7 and 9.2dB. Earlier estimated (see "Design Plan"), which indicated a minimum theoretical loss, had neglected some of the Fresnel effects. The figures for minimum loss are shown in Table 6. The predicted minimum is 4dB compared with the lowest measured value of 5.7dB and an average of 7dB. Random extra channel losses were introduced in fabrication as indicated by the departure from a smooth loss histogram. A smooth asymmetrical loss envelope with higher loss in the outer channels might be expected. Excessive outer channel loss arises from mode conversion and radiation bend loss, together with lower coupling efficiency into the waveguide mode resulting from increased lens aberration and launch obliquity. The asymmetry would reflect the poorer guidance at longer wavelengths. In retrospect, this suggest that the current concentrator design could be improved by using an asymmetric guide pattern with the straight guides corresponding to the longer wavelengths.

The results documented in Table 4 show channel loss increases between 1.0 and 2.2dB between room temperature and 50C. Between 0C and 20C, changes vary between -0.6 and 2.3dB, a much wider band with the lower channels showing the least change. It was not possible to establish the origin of these effects. Comparison of loss measurements made before temperature cycling and after completion reveals random differences probably representing experimental error with no systematic change evident. The temperature cycling has therefore not introduced any overall loss increase.

6.2 CHANNEL-CENTER WAVELENGTHS AND CHANNEL BANDWIDTHS

The data given in Table 5 shows that relatively large changes of between 2 and 3nm occur when the temperature is increased to 50C; all the wavelengths are slightly longer at this temperature. The absolute wavelength changes are too

large to be accommodated by the bandwidths of individual channels (2.4nm) and this problem would need further examination. At the same time, the average channel spacing, derived as an average of the first and last channel center wavelength also shows a small increase. At 0C, the channel center wavelengths are again slightly longer than at 20C, but there is no significant change in the average channel spacing. It may be deduced from the observed wavelength increases during both heating and cooling that there are at least two effects contributing to the temperature dispersion.

The accuracy with which the monochromator can be set to the peak channel signal is estimated to be ±0.05nm (not resolution-limited). The measurement error in channel separation is therefore ±0.1nm. Table 3 shows channel spacings which have a spread well above the measurement error. The variation was probably caused by small differences between waveguide positions introduced during fabrication.

The measured channel spacing of 7.2nm is below the design value owing to the parameter changes made necessary by the particular choice of lens. Substituting this value in equation (1) together with the values listed below enables the lens focal length to be determined.

d = 5 micron
D = 25 micron
θ = 8.92°

The value calculated is 17.1mm compared with the original design value of 13.2mm.

The wavelength span between channels 1 and 18 is 121.7nm in one unit and 122.8nm in the other, a difference of 1.1nm or 1% of the span. This indicates a small difference between the lens focal lengths in the units. The difference is about half that guaranteed by Ealing for matching. The channel loss measurements indicating a close correlation between the sum of the values for the individual units and the combined 'mux-demux' system also indicate that,

temperature considerations apart, the lenses can be matched to the required accuracy.

The measured channel bandwidth was 2.9nm, based on the half-power width and allowing for broadening from an estimated monochromator resolution of 0.5nm, the actual bandwidth would be 2.4nm. The channel spacing of 7.2nm and guide spacing of 25 micron would give a spot size of 8.3 micron, slightly above the original estimate of 8 micron.

6.3 CROSSTALK

Both far- and near-end crosstalks for a single multiplexer were orders of magnitude below the signal level at -60dB and at the limit of the detection system. With the two multiplexers connected through 5km of single mode fiber, end-to-end crosstalk levels below -25dB were measured.

6.4 POLARIZATION EFFECTS

The existence of any detectable polarization effects would have been surprising. The only intrinsic polarization-dependent loss mechanism is the very small difference in guide propagation loss between the TE and TM mode; this difference was so small that it would have been obscured by the general experimental scatter. The fibers used were not polarization maintaining and the elliptical polarization resulting at the concentrator would be randomly dependent on bends, which introduce strain birefringence in the cabled fiber.

6.5 FUTURE IMPROVEMENTS

Various measures could be taken to reduce multiplexer losses. The concentrator is one of the components which needs further development. In particular the handling procedures need to be reassessed, since both the top edges of the waveguides and the waveguide surfaces are easily damaged. The method used to assemble the input/output chip to the concentrator could be improved by using an out-of-contact assembly technique for the initial positioning to avoid dragging the silicon assembly across the surface. Alternatively it may be possible to protect the surface with a thick dielectric overlayer to bury the

waveguides. The introduction of a visual or IR technique to monitor transmission of the guides throughout fabrication and assembly would help to pinpoint weaknesses in procedure. Lastly, the redesign of the waveguide array to enable straighter guides to be used for the longer wavelength channels would probably be worthwhile.

The method of bringing out the fiber cable from the silicon V-groove arrays also needs examination. There are two weaknesses in the present arrangement. Firstly, with the loose fitting cabled fibers, any tension introduced by external bending can be transmitted to the V-groove array and may upset the optical alignment. Secondly, the use of a close-packed cable array within a cylindrical plug provided a neat method of producing a compact demountable and hermetic seal, but the transition from the linear array fibers to the close-packed cables presented some assembly problems especially with the need to avoid bend loss. It may be necessary either to extend the length of this transition or to maintain the linearity through the plug, possible with a double-decker arrangement of cables, at the expense of a bulkier plug design. Alternatively, the use of bulkhead connectors mounted on the multiplexer case might avoid some of these problems altogether.

The origins of the observed parameter changes with temperature have not been explored and further study is needed. Most likely sources are differential expansions either in the optical mounts or in the lens itself. Although the design of the flexure mounts minimized expansion, any small relative expansion between the flexure element and the screw adjuster could still be a problem. Residual expansion effects in a flexure mount could be investigated and balanced out by using an optical lever. The mounts could then be used in the multiplexer assembly with a mirror in place of the grating to investigate the effects of temperature on lens performance.

A more fundamental design change, could be considered to avoid some of the problems. The use of the Lipson-type construction with in-line waveguides for both the common and individual channels would simplify assembly and reduce the likelihood of waveguide surface damage, but at the probable expense of additional insertion loss.

7. SUMMARY AND CONCLUSIONS

The objective was to design, build and test prototype optical multiplexers to the requirements defined in the statement of work or agreed with RADC at the design stage. As shown in Table 7, these objectives were achieved. Some differences between the original design specifications and the final performance were attributable to the use, through necessity, of a less than optimum lens. There was a small scatter on the wavelength separation of individual channels, probably arising from waveguide fabrication variations. The scatter on the loss data would undoubtedly be reduced by further refinements to the assembly techniques. The near equivalence of the channel loss data for combined and separated units indicated the feasibility of matching focal lengths to the necessary accuracy.

Less definable were the temperature effects. A shift of 2 to 3nm occurred in the channel center wavelengths with one of the units at 50C. As the measured channel width was 2.4nm, it would be impracticable to use a mux-demux system maintaining this temperature difference between the units. The smaller shift noted when the unit was cooled to 0C could be accommodated within the bandwidth. The temperature sensitivity is indicative of the fine adjustments needed to tune the units. Identification of the sources of the mismatched expansion would require further investigations. Alternatively, means of thermally stabilizing the units could also be considered.

TABLE 7

Multiplexer Designed and Measured Parameters

DESIGN PARAMETERS	MEASURED PARAMETERS	COMMENTS
16-Channels	16-17 channels per unit	18 incorporated to allow for faults.
Operating range Centred on 1550nm	Range 1490-1610nm (Agreed with RADC)	Designed for DFB laser use.
Mux-demux system	16 operative channels	Yes, but not all adjacent.
Channel spacing 9nm	Channel spacing 7.2nm	Restricted by available lens and grating.
Channel bandwidth 3nm	Channel bandwidth 2.4nm	Restriction as above. Measurement limited by monochromator resolution.
Full spectral range 135nm	Average range 122.5nm	Depends on lens and grating.
Insertion loss/channel Minimum 2.9dB Maximum 6dB	 Minimum 5.7dB Maximum 9.2dB	 Values underestimated. Should have been min. 4dB, max. 7.1dB.
Optical Crosstalk Below -25dB	Below -60dB	Good wavelength channel isolation.

8. REFERENCES

[1] J Lipson, W J Minford, E J Murphy, T C Rice, R A Linke and G T Harvey "A Six-Channel Wavelength Multiplexer and Demultiplexer for Single Mode Systems", J. Lightwave Tech., LT-3, 5, 1159-62, Oct. 1985.

[2] E Bassous "Fabrication of Novel Three-Dimensional Microstructures by the Anistropic Etching of (100) and (110) Silicon", IEEE Trans. Electron Devices ED-25, 1178-1185, Oct. 1978.

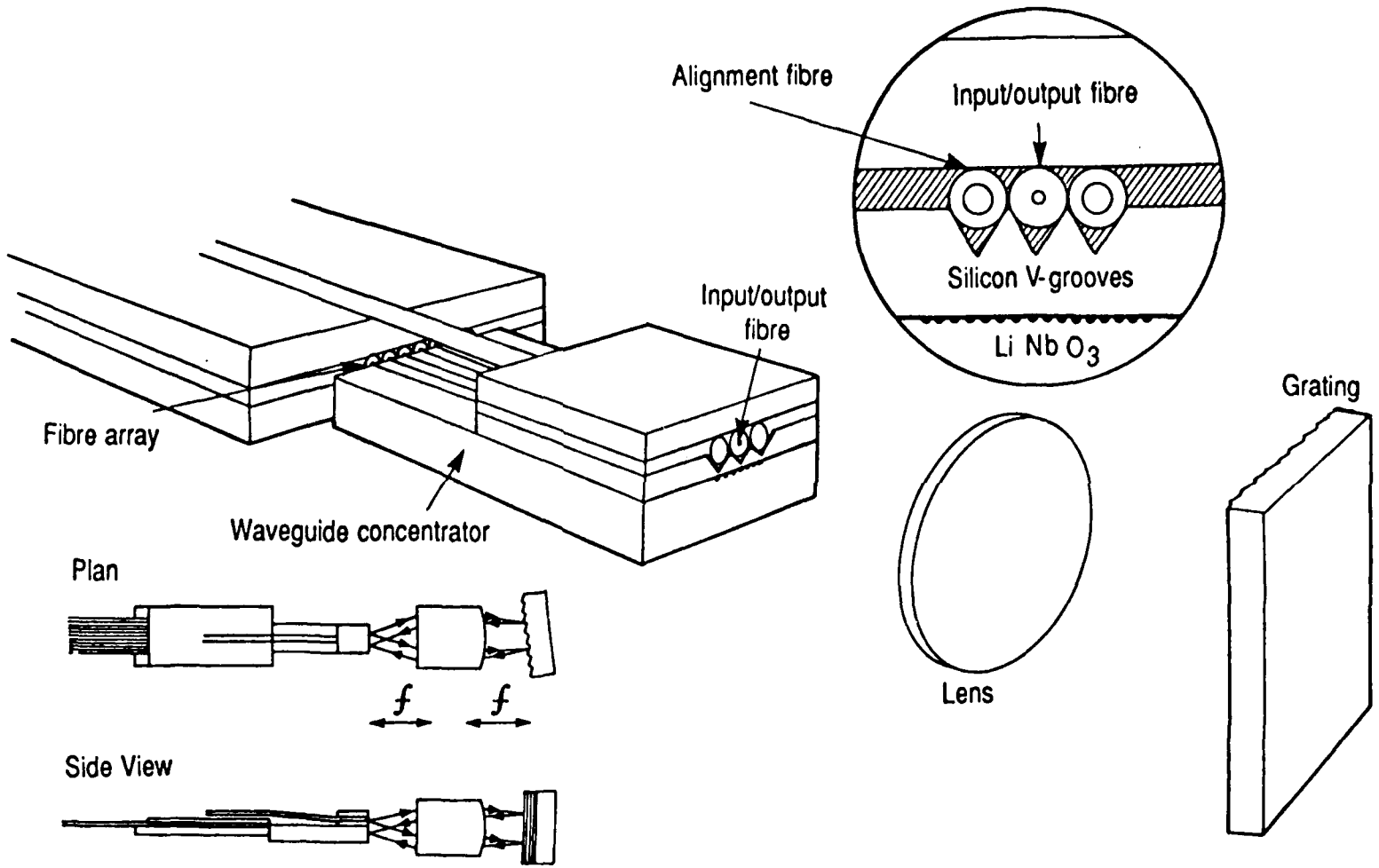

Fig. 1. WDM Design

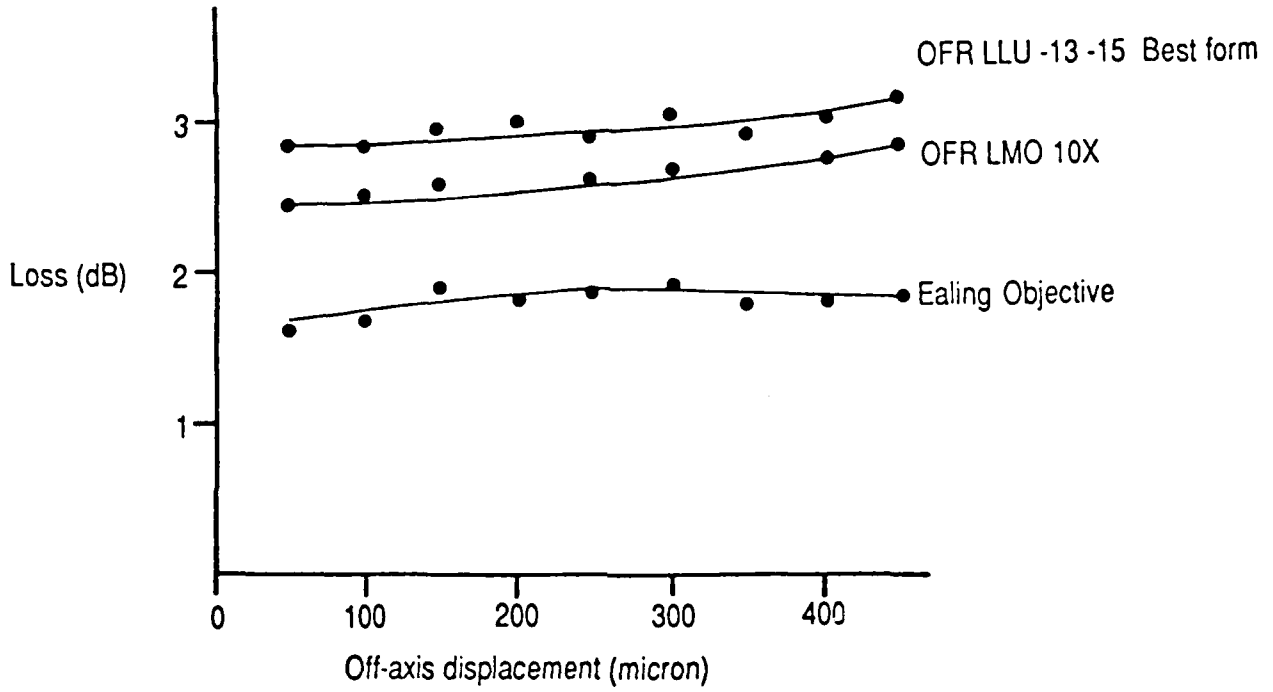

Fig. 2. Lens Evaluation

In transmission

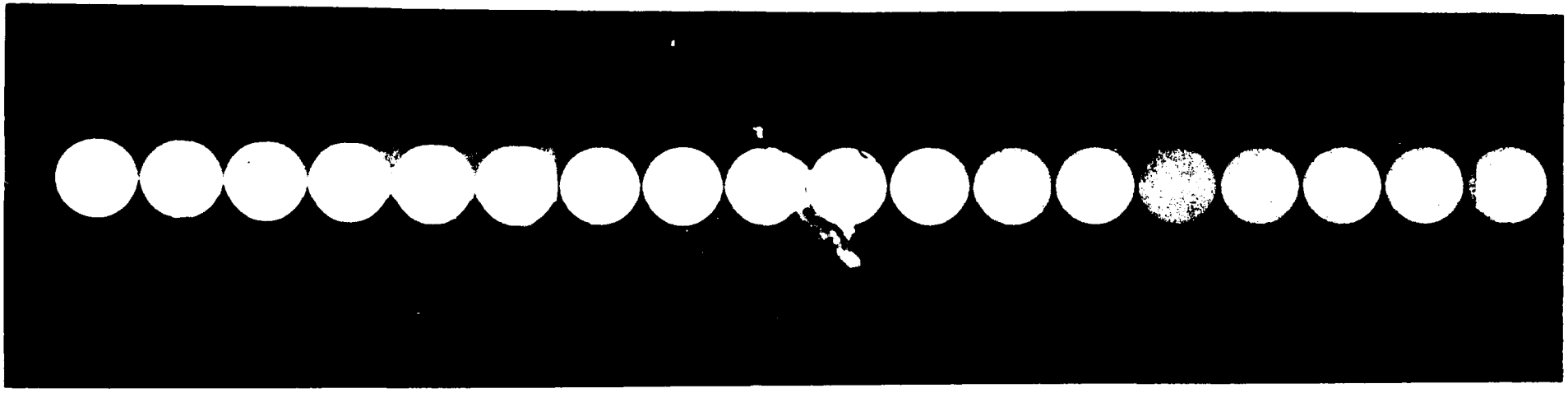

In reflection

Fig 3. 18 x 1 Single Mode Fiber Array

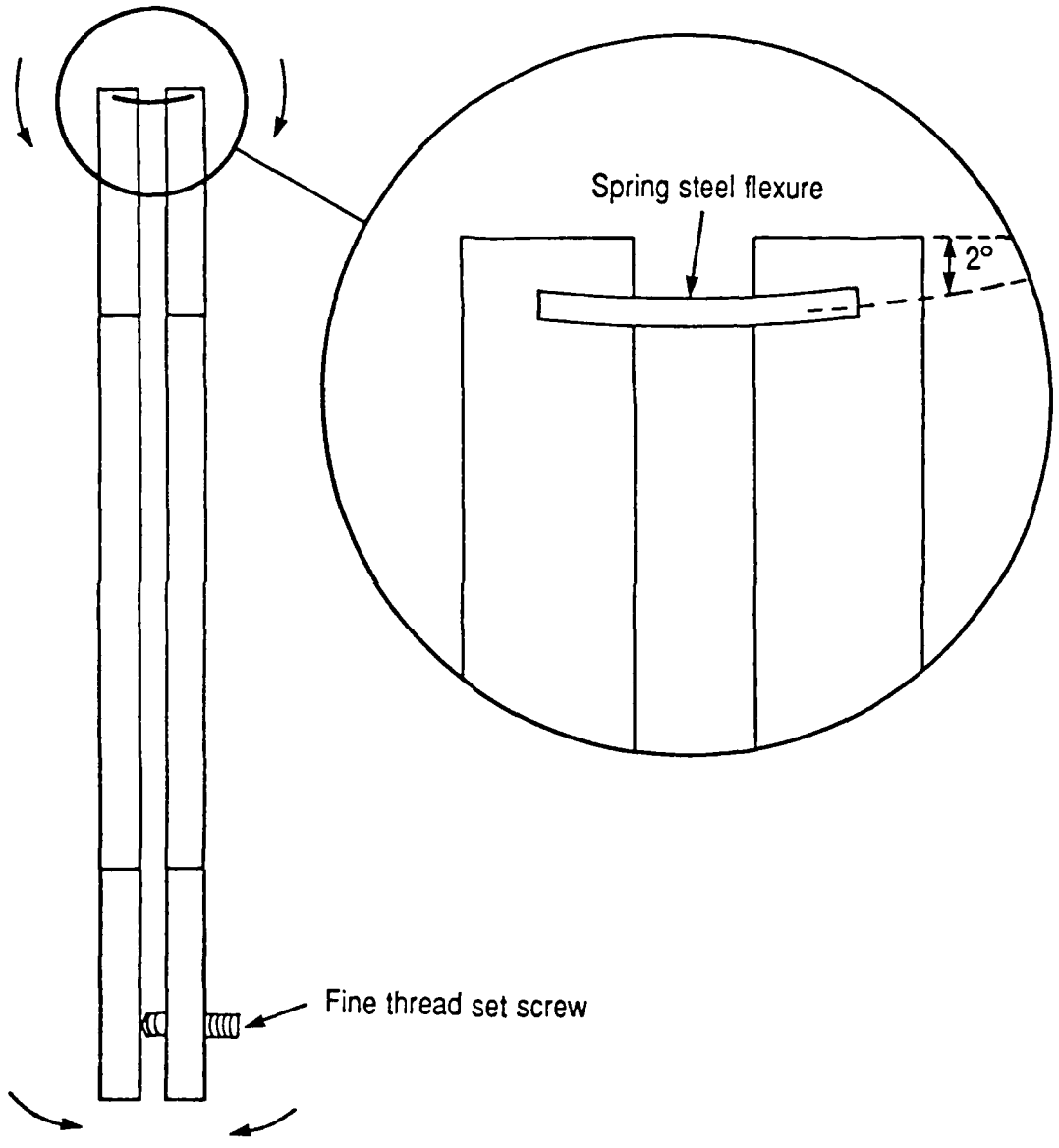

Fig. 4. Single Flexure Mount

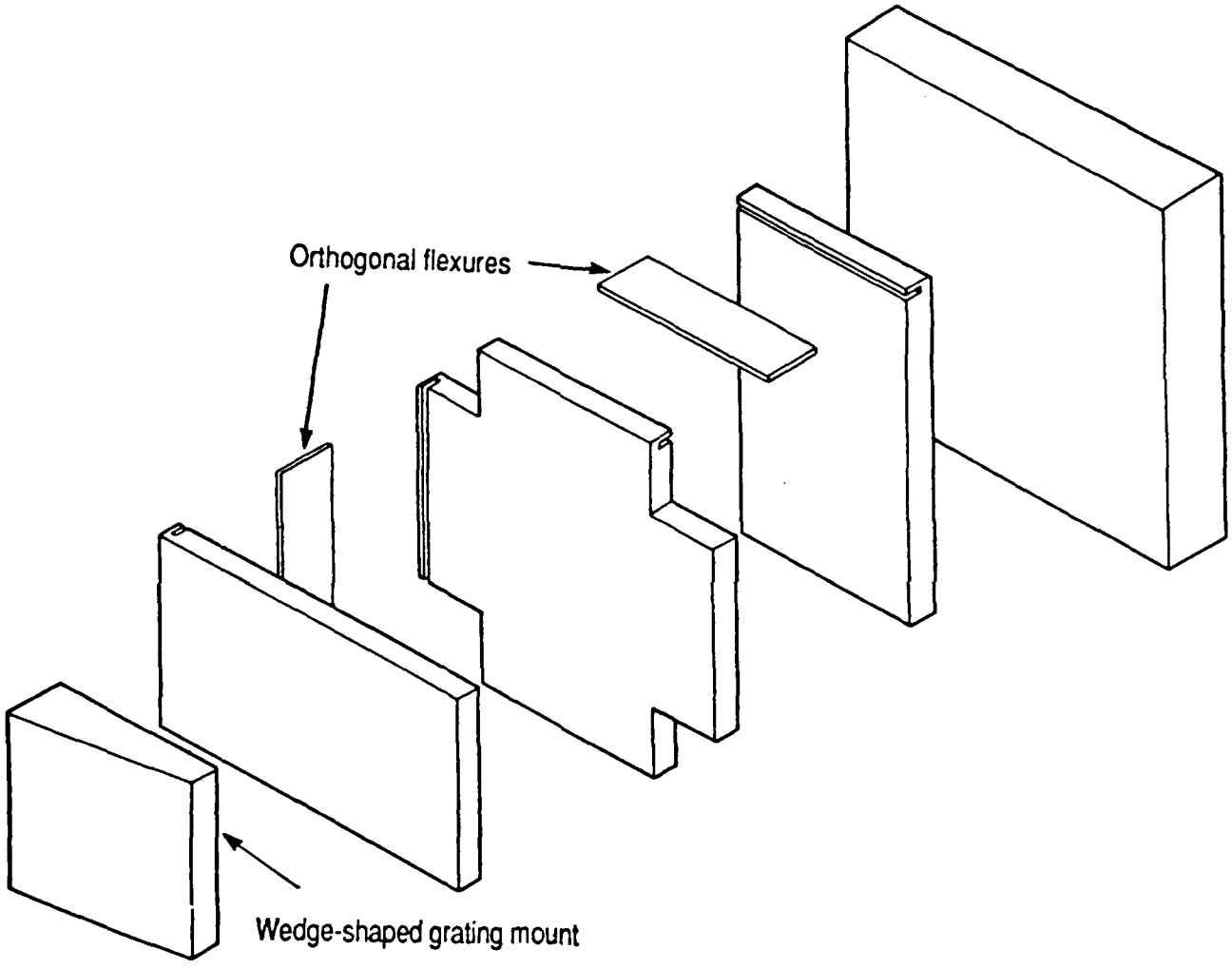

Fig. 5. Exploded View Grating Flexure Mount

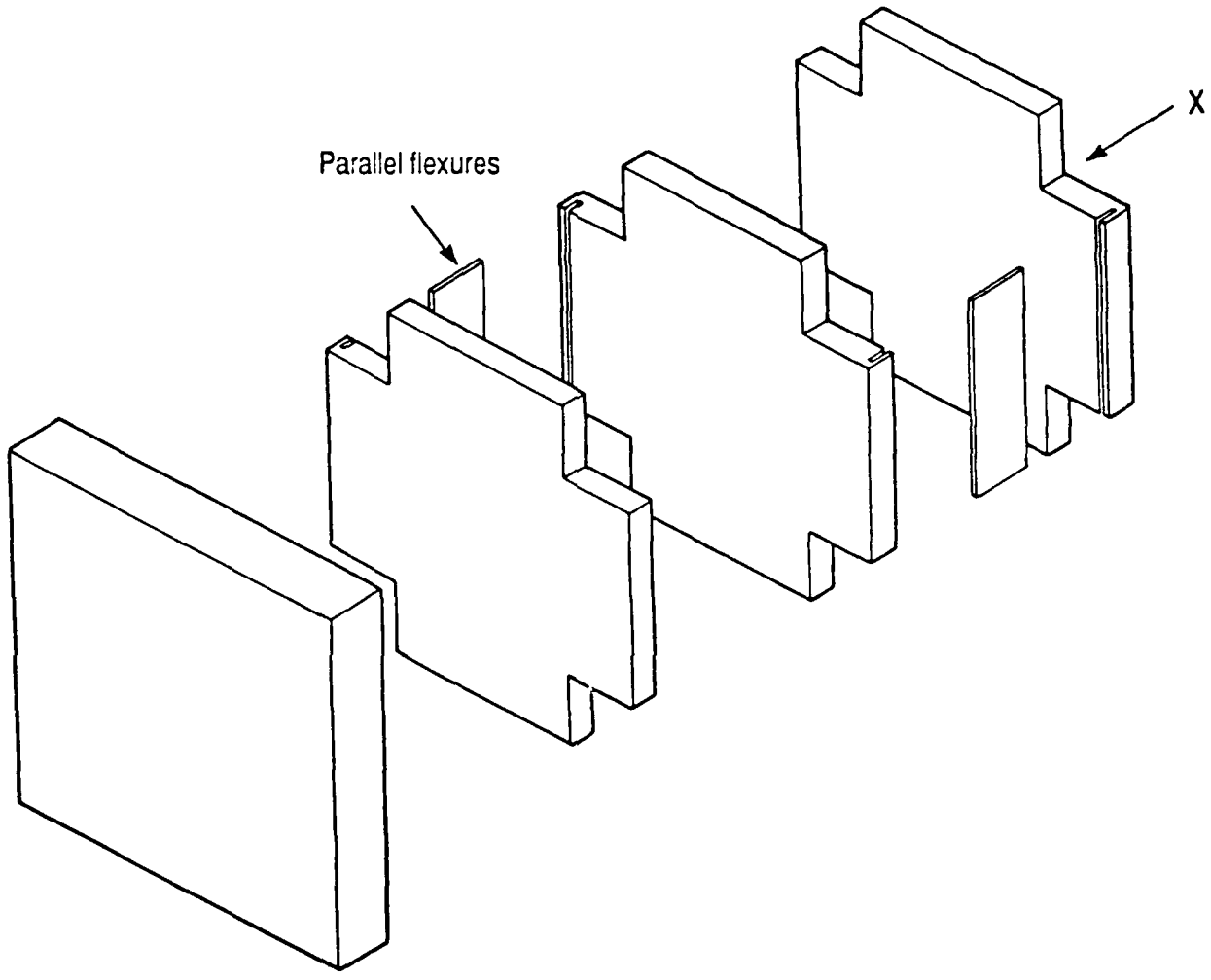

Fig. 6. Exploded View Lens Focusing Mechanism

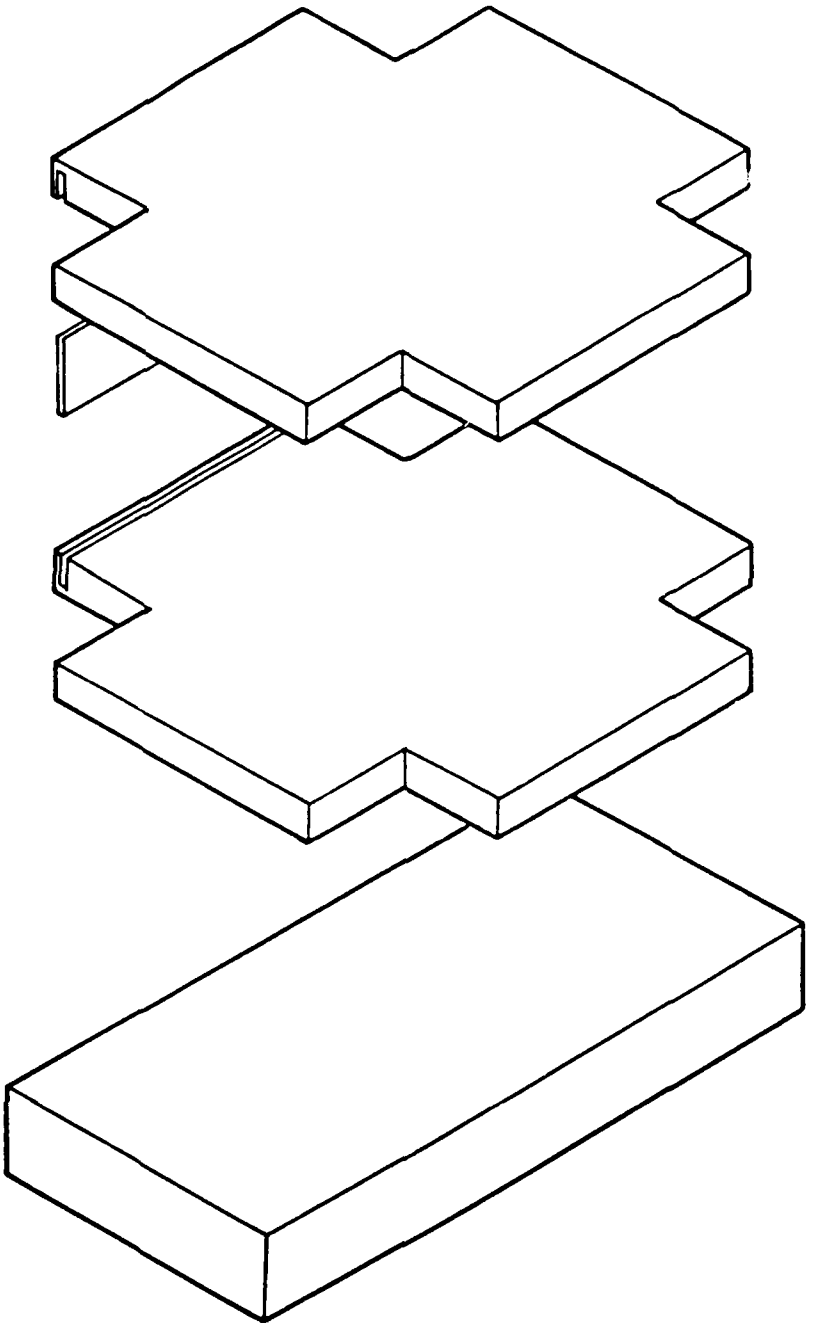

Fig. 7. Exploded View Concentrator Flexure Mount

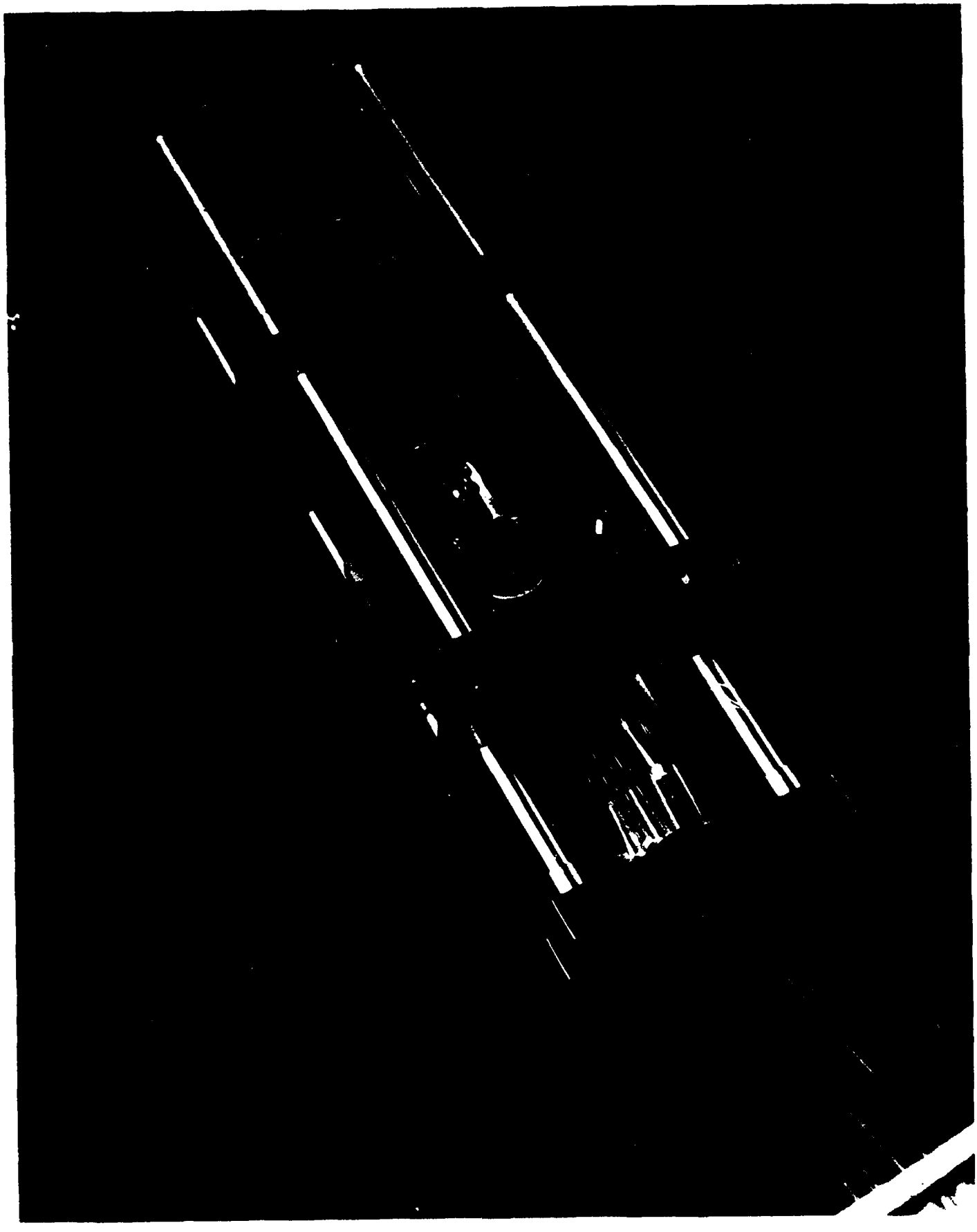

Fig 8. W.D.M. Assembly

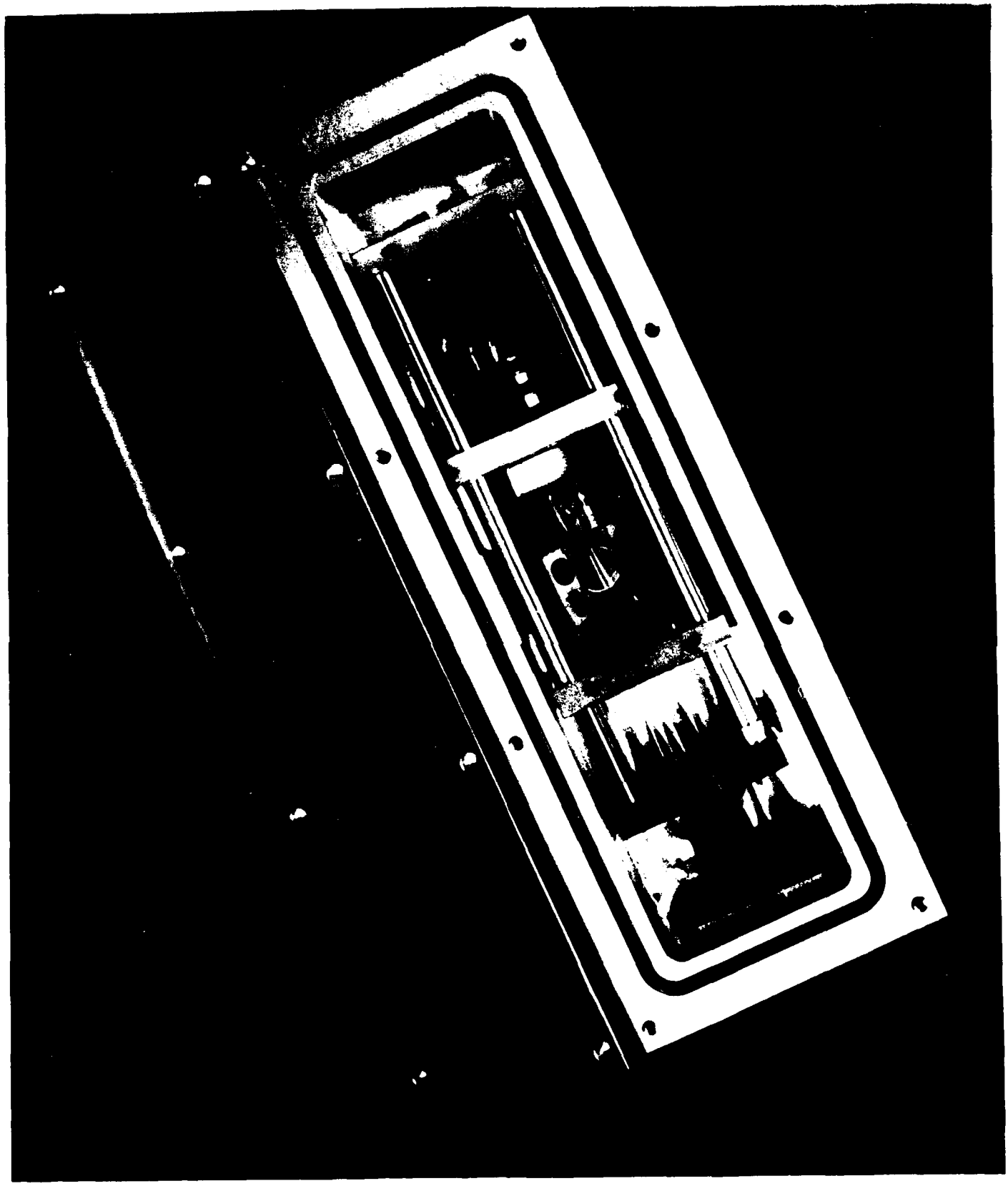

Fig 9. Case-Mounted W.D.M. Assembly

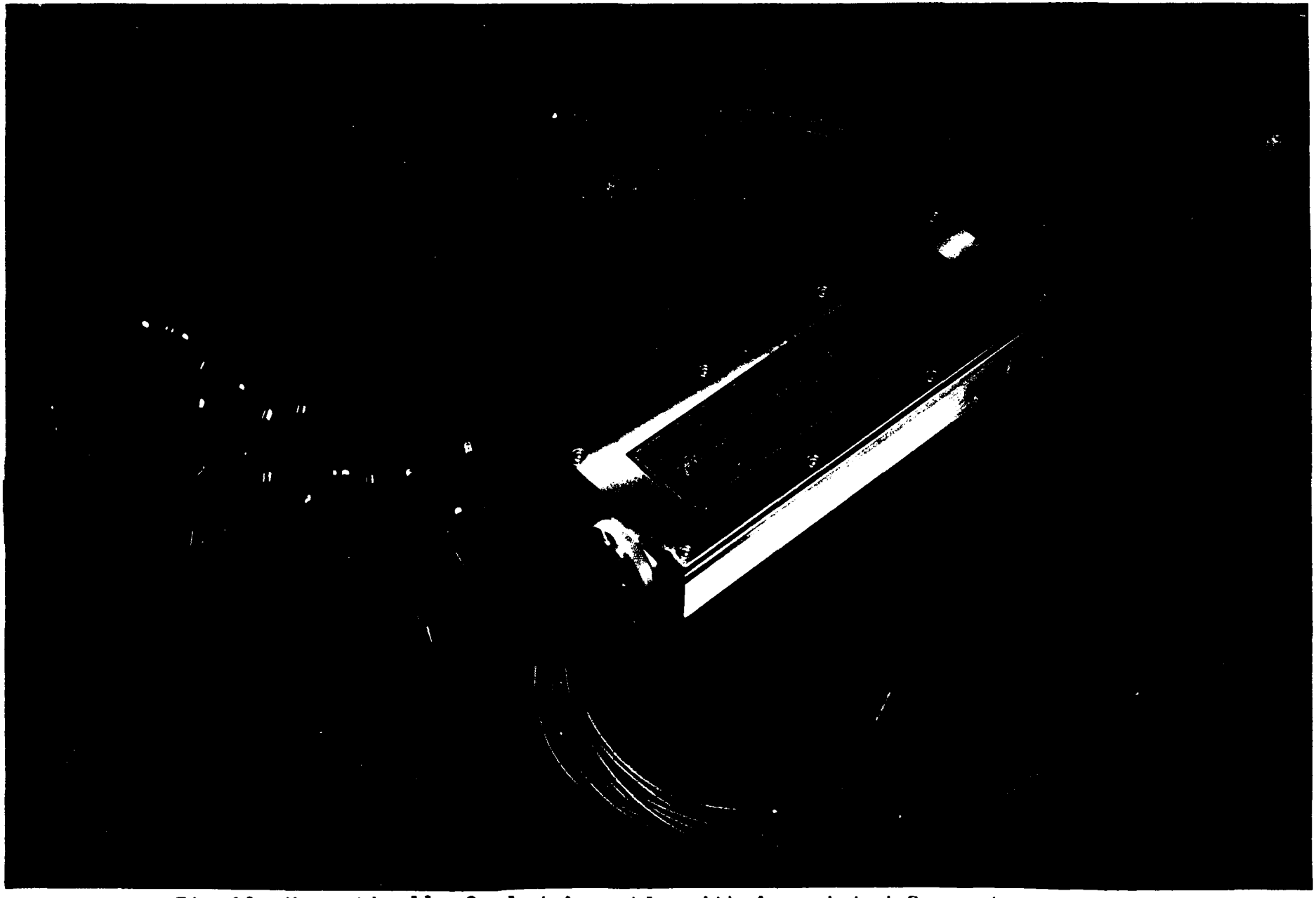

Fig 10. Hermetically-Sealed Assembly with Associated Connectors

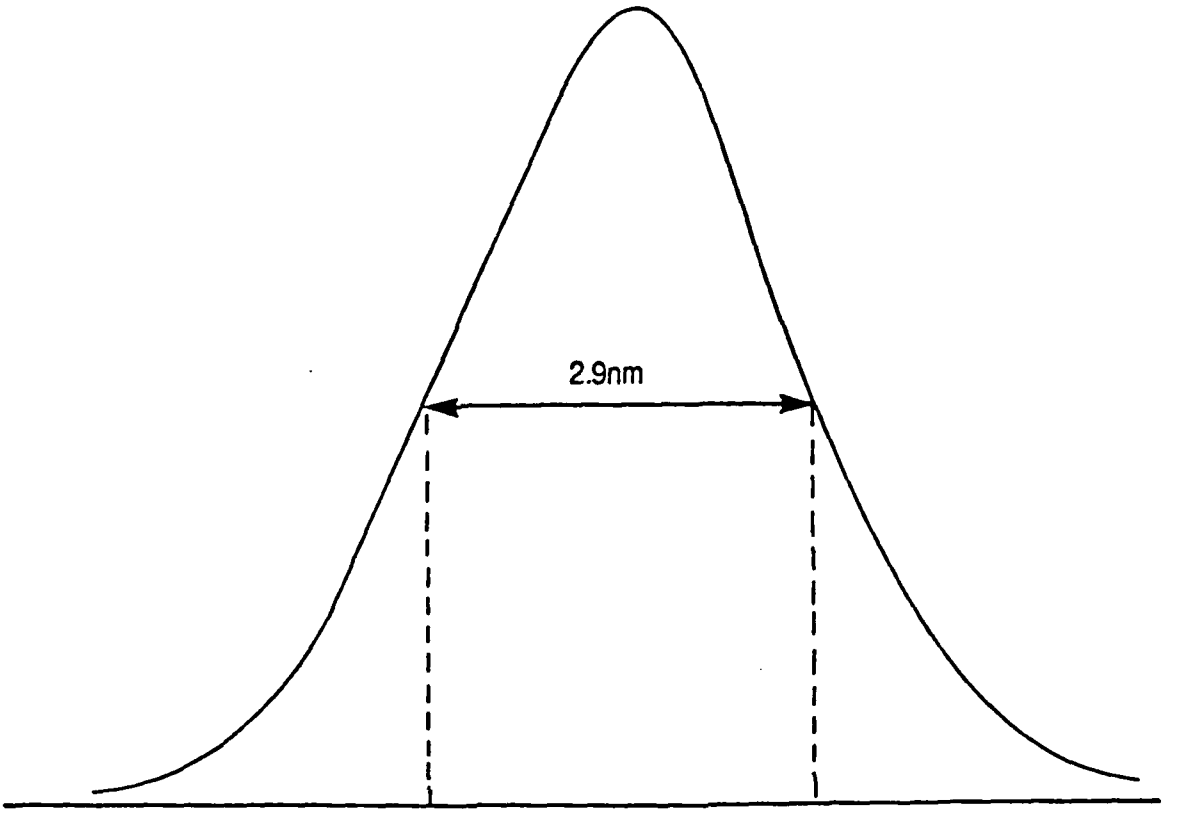

Fig. 11. Single Channel Wavelength Response

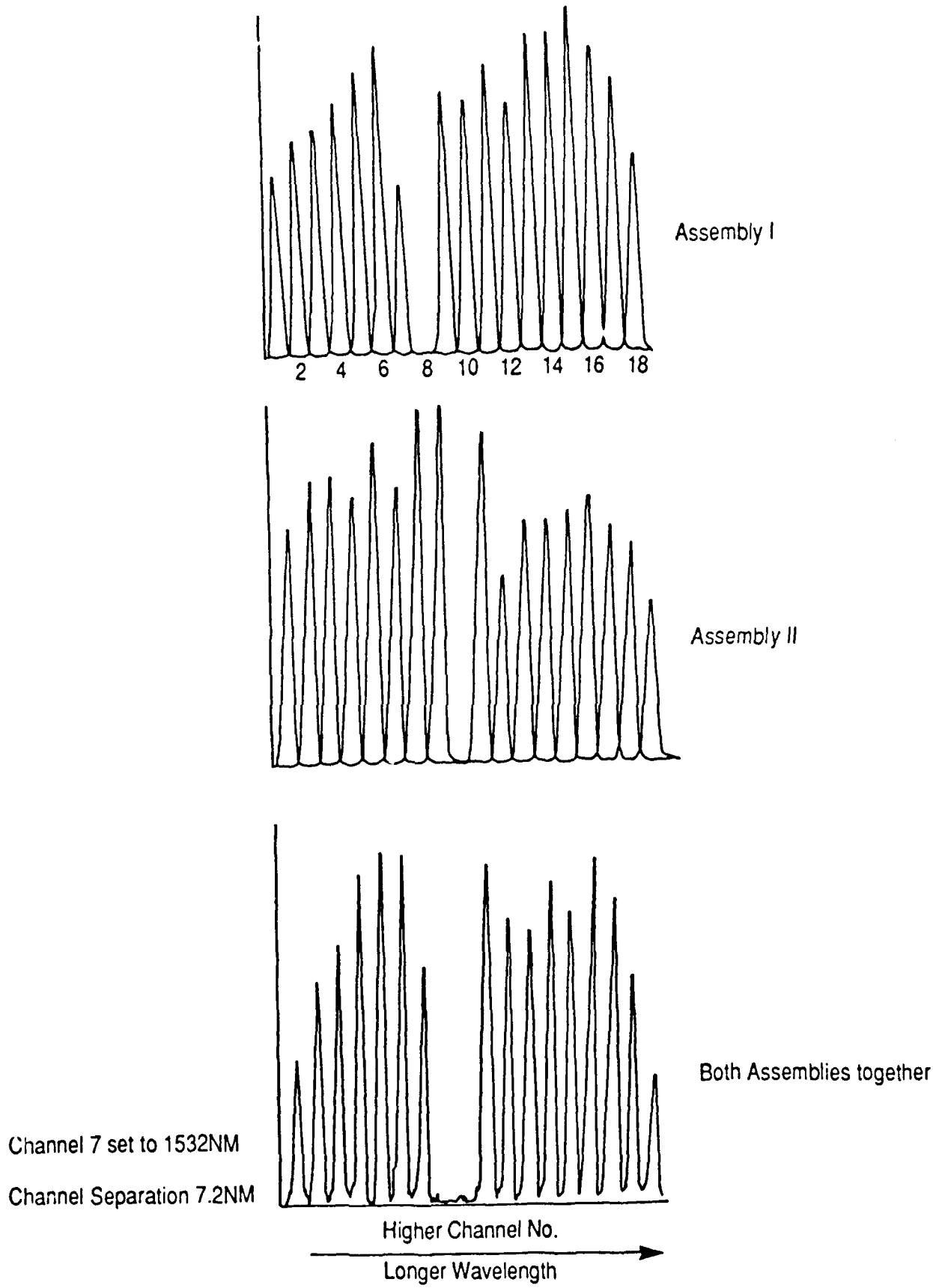

Fig. 12. Channel Wavelength Response Curves

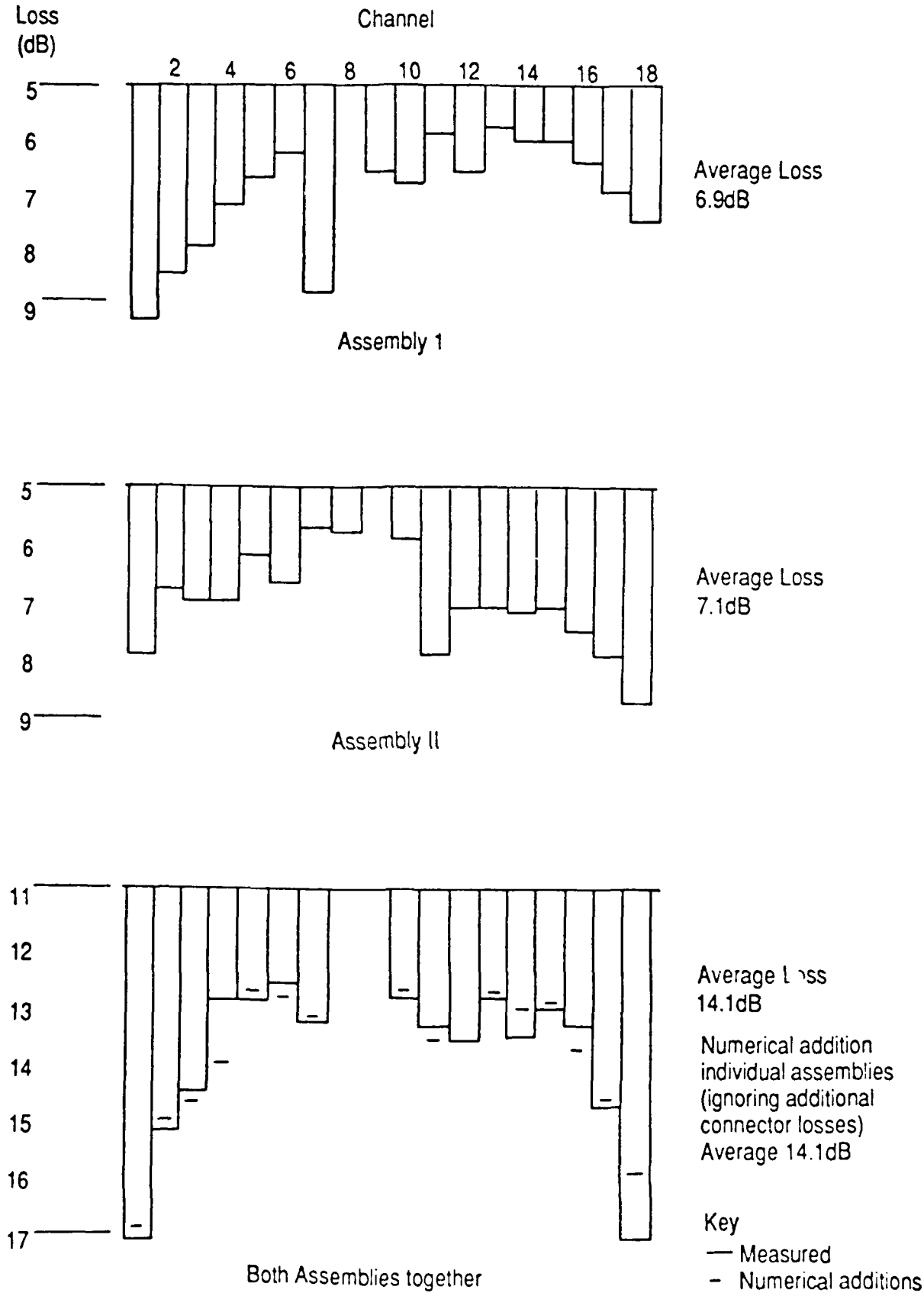

Fig. 13. Histograms of Channel Losses

MISSION
of
Rome Air Development Center

RADC plans and executes research, development, test and selected acquisition programs in support of Command, Control, Communications and Intelligence (C^3I) activities. Technical and engineering support within areas of competence is provided to ESD Program Offices (POs) and other ESD elements to perform effective acquisition of C^3I systems. The areas of technical competence include communications, command and control, battle management information processing, surveillance sensors, intelligence data collection and handling, solid state sciences, electromagnetics, and propagation, and electronic reliability/maintainability and compatibility.